Comprehensive characterization of osseous tissues from impedance measurements by effective medium approximation

Wenzuo Wei; Fukun Shi; Jie Zhuang; ... et. al

Check for updates

View Online

Export Citation

CrossMark

Articles You May Be Interested In

Convergence and stress analysis of the homogeneous structure of human femur bone during standing up condition

AIP Conference Proceedings (September 2017)

Estimation of femoral bone density from trabecular direct wave and cortical guided wave ultrasound velocities measured at the proximal femur in vivo

J Acoust Soc Am (May 2008)
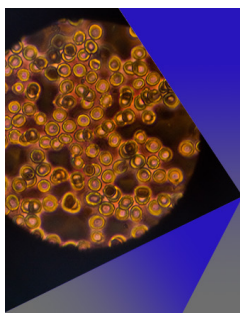
Comprehensive characterization of osseous tissues from impedance measurements by effective medium approximation

View Online   Export Citation   CrossMark

Wenzuo Wei,[1,2,3] (iD) Fukun Shi,[4] (iD) Jie Zhuang,[4] (iD) and Juergen F. Kolb[1,2,3,4,a)] (iD)

AFFILIATIONS

[1] Institute of Physics, University of Rostock, 18059 Rostock, Germany
[2] Department of Life, Light and Matter, University of Rostock, 18059 Rostock, Germany
[3] Leibniz Institute for Plasma Science and Technology (INP), 17489 Greifswald, Germany
[4] Suzhou Institute of Biomedical Engineering and Technology, Chinese Academy of Sciences, 215163 Suzhou, China

[a)]Author to whom correspondence should be addressed: juergen.kolb@inp-greifswald.de

ABSTRACT

A unified mixing (UM) model was developed to derive microstructural information of trabecular bone, i.e., bone volume fraction (BV/TV), from electrical impedance spectroscopy. A distinct advantage of the UM-model over traditional methods, such as equivalent circuit models and multivariate analysis, is that the influence of both the environment (hydroxyapatite) and different inclusions (water, fat, and air) can be taken into account simultaneously. In addition, interactions between the different components such as interfacial polarization can be addressed by a dedicated fitting parameter v. Accordingly, values of BV/TV for different bone samples, e.g., including or not including water, were determined in the higher frequency range of 1–5 MHz. Results showed good agreement with experimental data obtained by micro-computer tomography. In particular, predictions for dielectric parameters that were derived for 3 and 4 MHz were found most promising for the assessment and distinction of osteopathic conditions and differences. This was shown by a clear differentiation of osseous tissues, e.g., the greater trochanter, femoral head, and femoral neck.

I. INTRODUCTION

Common technologies for the diagnosis of bone conditions, e.g., micro-computer tomography (μCT) and dual-energy x-ray absorptiometry (DXA), are associated with high equipment cost and other disadvantages, such as radiation exposure. Electrical impedance spectroscopy (EIS) as a non-invasive, real-time, and cost-effective method offers a different approach and a potentially clinical alternative.[1–5] This technique has already been used to study the dielectric properties of osseous tissues, such as permittivity and conductivity, and attempts have been made to correlate these parameters with the bone microstructure that was foremost determined by bone mineral density (BMD) or the bone volume fraction (BV/TV). Both parameters provide diagnostic information about bone stiffness and bone quality as an indicator of osteopathy, e.g., micro-fractures and osteoporosis.[6,7] In addition, the impedance

properties were also found to be dependent on the associated components, such as water and fat. Therefore, microstructural information (BV/TV) and compositions of osseous tissues could be explored with the assistance of EIS if a sensitive correlation with their dielectric properties could be established. However, this requires a more reliable and unambiguous classification of permittivities and conductivities with respect to different microstructures[8] and pathological statuses[9] than is currently available.

Common methods for the interpretation of dielectric properties included electrical circuit models (ECMs) or Cole models and multivariate analysis, e.g., principle component analysis (PCA) or linear discriminant analysis (LDA). However, a convincing multivariate analysis is subject to a big sample size and further suffers from the lack of any relation to underlying physical processes. The physical interpretation that could be derived from ECM elements, e.g., Cole parameters, was prone to large errors due to limitations

in the assumptions of the underlying model and conjectures on initial values for each element. Therefore, the associated interpretation of characteristics of dielectric data remains ambiguous.[10,11] More general, purely statistical, treatments of the correlation with the microstructure and composition were afflicted by similar issues in the understanding of impedance properties of bone tissues.

Accordingly, previous studies, employing these different approaches, have yielded contradictory relationships between dielectric properties and BV/TV or composition, e.g., water- or fat-content. In addition, many of these studies were rather selective in the frequencies that were evaluated from impedance spectra or in scope, i.e., with respect to constituents and parameters that had been considered. Moreover, a large number of samples, which is required in order to derive any meaningful correlation at all, was not necessarily available. Unal *et al.* indicated a relationship between dielectric properties, i.e., permittivity and conductivity, with bound water ($R^2 \geq 0.5$) at low frequencies (0.5–1 MHz) for cortical bone.[12] Balmer *et al.* correlated conductivity and BV/TV ($R^2 = 0.83$) for impedance measurements at 100 kHz for bovine bone samples *ex vivo*.[2] Sierpowska *et al.* obtained a positive correlation (r = 0.68) between permittivity and BV/TV and a negative relationship with conductivity (r = −0.59) for trabecular bone at 1.2 MHz.[13] However, Meaney *et al.*[14] indicated a negative correlation (r = −0.6) between permittivity and BV/TV at 1.3 GHz, while Amin *et al.* obtained a weak positive correlation with conductivity at 900 MHz for diseased bones.[15] Consequently, an unequivocal relationship between compositions and microstructure (BV/TV) and dielectric properties is promising to determine the bone status via impedance measurements; however, the so far inconsistent results cannot provide a convincing general correlation. Accordingly, advanced methods are obviously necessary for a better understanding and interpretation of impedance properties of osseous tissues as a mandatory prerequisite for any clinically relevant application.

An evaluation of impedance measurements by effective medium approximations (EMAs) offers a solution. The approach describes the distribution of different components, i.e., inclusions, in a system, i.e., environment, and the effect of individual physical characteristics on the bulk properties of the system. Possible interactions between inclusions and with the environment are explicitly included. An example is the Bruggeman model, which was an attempt to relate microstructural information on osseous tissue with impedance properties.[16] This model, however, might yield conflicting results, in particular, for a large volume fraction of inclusions and a large contrast between the dielectric properties of environment and inclusions,[17,18] which is, for example, the case if the inclusions are filled with water. In comparison, a unified mixing (UM) model can take the microstructure and different compositions with different dielectric properties into account simultaneously.[19] Furthermore, the UM-model utilizes the prior knowledge on the system and regards the main component of the bone, i.e., hydroxyapatite (HA), as the "environment" while other components are described as "inclusions." This is decidedly different from the Bruggeman model, which treats all inclusions symmetrically. In the UM-model, the effect from the large contrast of volume fractions of different components and their possible interaction, which could affect the derivation of microstructural information, can be accounted for by a fitting parameter, ν.[19] The good agreement between the estimated results at a specific frequency and the experimental data that was

determined by μCT confirmed the applicability and effectiveness of the model.

II. METHODS

The development of a UM-model was based on a comparison of values that were determined for BV/TV for different sites of porcine trabecular bone by μCT-imaging with predictions based on the assessment of electrical impedance measurements. First, bone samples were prepared from different regions of the bones. Subsequently, impedance measurements were conducted on these samples, from which dielectric properties (relative permittivity and conductivity) were derived as bulk material properties independent of their geometry and particularly their thickness. Volume fractions of water and fat that the UM-model required were quantified, and the respective contribution to the impedance of individual samples (e.g., with or without fat content) was studied. Eventually, values for BV/TV were derived from the UM-model by considering the volume fractions for different compositions and their corresponding permittivity. These results were compared with data derived for BV/TV from μCT-images for a statistical assessment of the accuracy of the predictions.

A. Sample preparation

Bone samples were prepared from the femurs of six female Landrace pigs (200.17 ± 15.18 kg) that were raised by the Research Institute for Farm Animal Biology (FBN), which were processed within 24 h post-mortem. Sample preparation was previously described in detail.[20] In brief, after the extraneous tissue was removed, rough thin slices from different regions were cut with a band saw (Epple Metallbandsäge BS 125 GS, Epple Maschinen GmbH, Germany), perpendicular to the major axis of the investigated anatomical regions. Discs 20 mm in diameter were then extracted with a hollow drill. Afterward, the rough top and bottom surfaces were smoothened with sandpapers of different grit sizes to a final thickness of ~1.3 mm. To ensure good contact with the electrodes of the impedance diagnostic system, sufficient parallelity of the surfaces was ensured. The discs were subsequently ultrasonically cleaned in 0.9% NaCl-solution. The cleaning time was set to 3 min in order to remove most of the remaining debris, possible residual blood, and to not damage the samples. The specimens were then frozen at −20 °C in aqueous solutions with 0.9% NaCl until needed for measurements. A total of 72 samples were prepared from different anatomical sites (Fig. 1), i.e., 24 for each region, including the greater trochanter (PFGT), femoral head (PFH), and femoral neck (PFN), with their thickness shown in Table I. The similarly raised pigs and close-by anatomical regions were deliberately chosen to develop a UM-model with high sensitivity for even small anatomical differences.

B. Characterization of composition and microstructure

The major component of the osseous tissue comprised the inorganic phase, i.e., hydroxyapatite (HA). The wet samples, cut from the bone, included air (pores that were not filled otherwise), soft tissue (primarily fat), and water. The different components were successively removed, i.e., first water and then fat, to assess their influence on the impedance measurements.
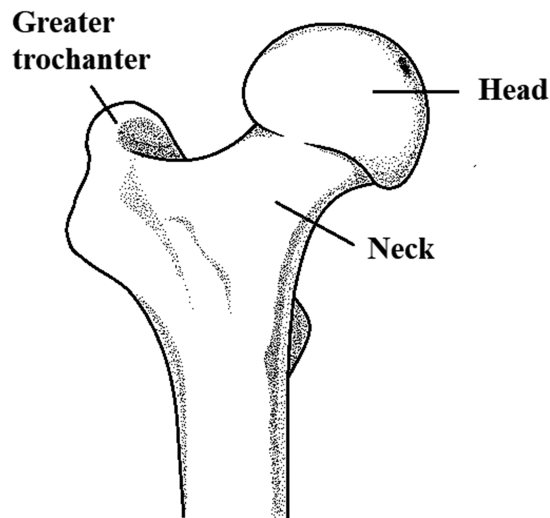
FIG. 1. Anatomy of porcine trabecular bone and the regions investigated in the study, including the greater trochanter (PFGT), femoral head (PFH), and femoral neck (PFN).

To remove water from wet samples, they were stored in a desiccator, connected to a vacuum pump, after thawing. The drying time was set to 24 h because the weight of the samples, which included fat (fat-retained samples), remained unchanged from this time onward. The removed water content, W_{cont}, was calculated from the difference between wet (W_{wet}) and dry weight (W_{dry}), according to

$$W_{cont} = \frac{W_{wet} - W_{dry}}{W_{wet}}. \tag{1}$$

To remove fat, fat-retained samples were ultrasonically cleaned in acetone. The cleaning time was 14 min to ensure that the fat was removed and excessive damage to the samples, such as erosion of HA, was avoided. Acetone was then evaporated at room temperature for 10 min to get the net fat-free weight of the now dry samples. Quantification of the fat content, F_{cont}, was obtained from the weight difference of the samples before (W_{dry}) and after immersion in acetone ($W_{fat\text{-}free}$), as described by

$$F_{cont} = \frac{W_{dry} - W_{fat-free}}{W_{dry}}. \tag{2}$$

Water- and fat-content for each region, which were determined according to Eqs. (1) and (2), respectively, i.e., mean values and standard deviations with respect to different bone regions, are shown in Table II.

TABLE I. Thickness of the prepared bone tissue samples.

Anatomical region	PFGT	PFH	PFN
Thickness (mm)	1.33 ± 0.19	1.36 ± 0.21	1.38 ± 0.13

TABLE II. Average relative contribution of water and fat [determined from Eq. (1) and Eq. (2), respectively] and bone volume fraction, BV/TV (determined from μCT-images) of the samples from different anatomical sites.

Bone region	PFGT	PFH	PFN
Water content, W_{cont}	0.14 ± 0.02	0.13 ± 0.02	0.18 ± 0.07
Fat content, F_{cont}	0.44 ± 0.06	0.26 ± 0.10	0.27 ± 0.07
BV/TV	0.29 ± 0.03	0.40 ± 0.06	0.35 ± 0.05

The microstructure can be quantified by the bone volume fraction, BV/TV, expressing the ratio of bone volume to total tissue volume, i.e., sample volume. Sample scanning was performed by micro-computed tomography (microCT, Skyscan 1076, Bruker, USA) with a resolution of 9 μm. After scanning, the reconstruction of images for each sample was conducted with the *NRecon* software.[21] To avoid edge effects, a region of interest (ROI) was identified in the middle of the images with the *CTAn* software (Version 1.10).[22] Afterward, ROI-images were segmented into binary images by using the *Global Threshold* method built into *CTAn*. Examples of images for each step of the analysis are shown in the flowchart of Fig. 2. Microstructural parameters, e.g., BV/TV, were calculated automatically based on the 3D-mode of *CTAn*. The average values of BV/TV for each region have been summarized in Table II. Note that all regions showed a significant distinction ($p < 0.01$) for different components (water and fat) and BV/TV.

C. Relative permittivity and conductivity

Samples were thawed at room temperature just prior to impedance analysis. Extraneous liquid on the surfaces of samples was removed by wiping them clean with paper towels, especially to reduce electrode polarization (EP). The impedance properties were first determined from 100 Hz to 5 MHz using a high-precision impedance analyzer (Agilent 4294A, Agilent Technologies Japan Ltd., Murotani, Kobeshinishiku, Japan) in a parallel capacitor configuration (Agilent 16451B, Keysight Technologies, Japan). The three-electrode design of the parallel capacitor is able to account for stray capacitance and, therefore, can reduce measurement errors. In addition, calibrations, including open- and short-circuit compensation, were performed for the Agilent analyzer and the electrode configuration according to operational instructions.[23] An AC-excitation signal of 200 mV was applied in all experiments. To ensure the reproducibility and accuracy of results, each sample was repositioned and measured four times. Afterward, the dielectric properties, e.g., relative permittivity, of the samples were determined by considering their geometry, i.e., size, together with the obtained complex impedance values.

Dielectric parameters for the individual main components, i.e., hydroxyapatite, fat, and water, of the investigated osseous tissue were evaluated with respect to different frequencies. For HA, a relative permittivity of 50 was derived experimentally for a frequency of 1 MHz, in good agreement with the literature.[16,24] A relative permittivity of 43 was assumed for fat at higher frequencies (above 3 MHz).[25] For air and water, relative permittivities could be considered static at room temperature and for the investigated frequency range, with values of 1 and 80, respectively.[26]
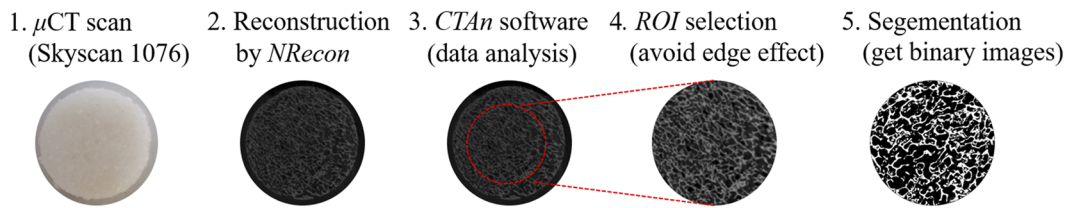
FIG. 2. Steps for the determination of microstructural parameters, i.e., BV/TV, from the analysis of μCT-images.

D. Unified mixing (UM) model

An effective medium approximation (EMA), or effective medium theory, is generally a homogenization model to describe, i.e., approximate, inhomogeneous and anisotropic composite materials. Rather than simply averaging the values of individual constituents, EMAs can, for example, derive bulk dielectric properties, i.e., relative permittivity, of a composite based on specific characteristics and distributions of components, i.e., inclusions in a specific environment, and the corresponding relative volume fractions for each inclusion. As a simple homogenization principle, it has been applied to predict the macro-properties of different complex materials[27] and biological tissues,[28] including bones.[16,29] So far, for this purpose, EMA-models, including the Maxwell Garnett model and Bruggeman model, were used, which would yield predictions that differed considerably from the actual system-properties if there was a high contrast of the permittivities of the environment and inclusions.[18] In this study, the issue could be addressed by an EMA, which was based on the Unified Mixing (UM) formula, hence the unified mixing model, for the different components of the system,[19]

$$\frac{\varepsilon_{eff} - \varepsilon_e}{\varepsilon_{eff} + 2\varepsilon_e + \nu(\varepsilon_{eff} - \varepsilon_e)} = \sum_{i=1}^{n} f_i \frac{\varepsilon_i - \varepsilon_e}{\varepsilon_i + 2\varepsilon_e + \nu(\varepsilon_{eff} - \varepsilon_e)}. \quad (3)$$

Here, ε_{eff} denotes the bulk effective permittivity of bone tissue, ε_e and ε_i describe the permittivity of HA, designated as the environment, and the ith inclusion, respectively, with the corresponding relative volume fraction, f_i. The significant inclusions were water, fat, and air. As literally indicated by "unified" and "mixing," the model considers, on the one hand, the contribution from each component and their corresponding relative volume fraction to the bulk properties. On the other hand, the dimensionless parameter ν accounts for the polarization of inclusions,[19] which are specifically correlated also with respective interfaces.

E. Statistical analysis

To exclude the contribution of EP to the analysis of dielectric parameters at lower frequencies, the bulk relative permittivity, ε_{eff}, for each sample was deduced from impedance measurements at higher frequencies, i.e., 1, 2, 3, 4, and 5 MHz. Appropriate values for ν (>0) had to be determined for these frequencies to derive BV/TV or dielectric properties for each sample from the UM-model. The parameter ν can be estimated by a cost function according to Eq. (4) with respect to the experimentally determined BV/TV from μCT-images, i.e., $f_{\mu CT}$, and corresponding model data, i.e., f_{HA},

$$\min \sum_{j=1}^{5} \cos t = \min\left(\frac{1}{5}\sum_{j=1}^{5}|f_{\mu CT} - f_{HA}|\right). \quad (4)$$

Here, j refers to the five distinct frequencies from 1 to 5 MHz that were the basis of the impedance analysis. The *minimize*-function that is included in the Python library *Scipy* was used to find the most suitable values for ν that resulted in minimum errors. After the determination of ν, BV/TV or relative permittivity can be estimated for each sample. Notably, the derived values for ν were not necessarily integers.

Impedance measurements were conducted four times for each sample (see above), and relative permittivity was calculated by considering their thickness. Mean values (mean) and standard deviations (SDs) were calculated by built-in libraries of *Python*. A Pearson correlation was applied to determine the correlation coefficients between BV/TV and the parameters of the UM-model, i.e., ν. Statistical significances were evaluated with a t-test.

III. RESULTS

A. Electrical impedance of porcine trabecular bone

Bode plots, including impedance and the phase angle, are shown in Fig. 3 for dry samples [Figs. 3(a) and 3(b)], fat-retained samples without water but still containing fat [Figs. 3(c) and 3(d)], and samples of the originally extracted bone, i.e., wet samples [Figs. 3(e) and 3(f)], for different sites, i.e., PFGT, PFH, and PFN. As expected, the impedance spectra were strongly frequency-dependent, and impedance decreased with frequency, where a larger standard deviation was observed for measurements at lower frequencies than at higher frequencies. The decrease was particularly significant for dry and fat-retained samples where the impedance exceeded 10^8 Ω at low frequencies, which then fell off for all the regions to less than 10^5 Ω at frequencies higher than 3 MHz [Figs. 3(a) and 3(c)]. The phase angle was found between $38°$–$46°$ at 100 Hz and increased to $87°$ at 5 MHz for all regions [Figs. 3(b) and 3(d)]. No obvious differences were observed for impedances and phase angles between dry and fat-retained samples for the different regions. Only a slight but insignificant difference at frequencies lower than 10^4 Hz could be distinguished [Figs. 3(c) and 3(d)].

Unsurprisingly, impedances were significantly lower for wet samples [Fig. 3(e)] than for dry and fat-retained samples. Standard deviations were more pronounced for the investigated frequencies but still smaller than those for dry and fat-retained samples in terms of magnitude. Mean values dropped for impedances from about 4 kΩ at 100 Hz to 1.6 kΩ at 5 MHz with a slight difference between
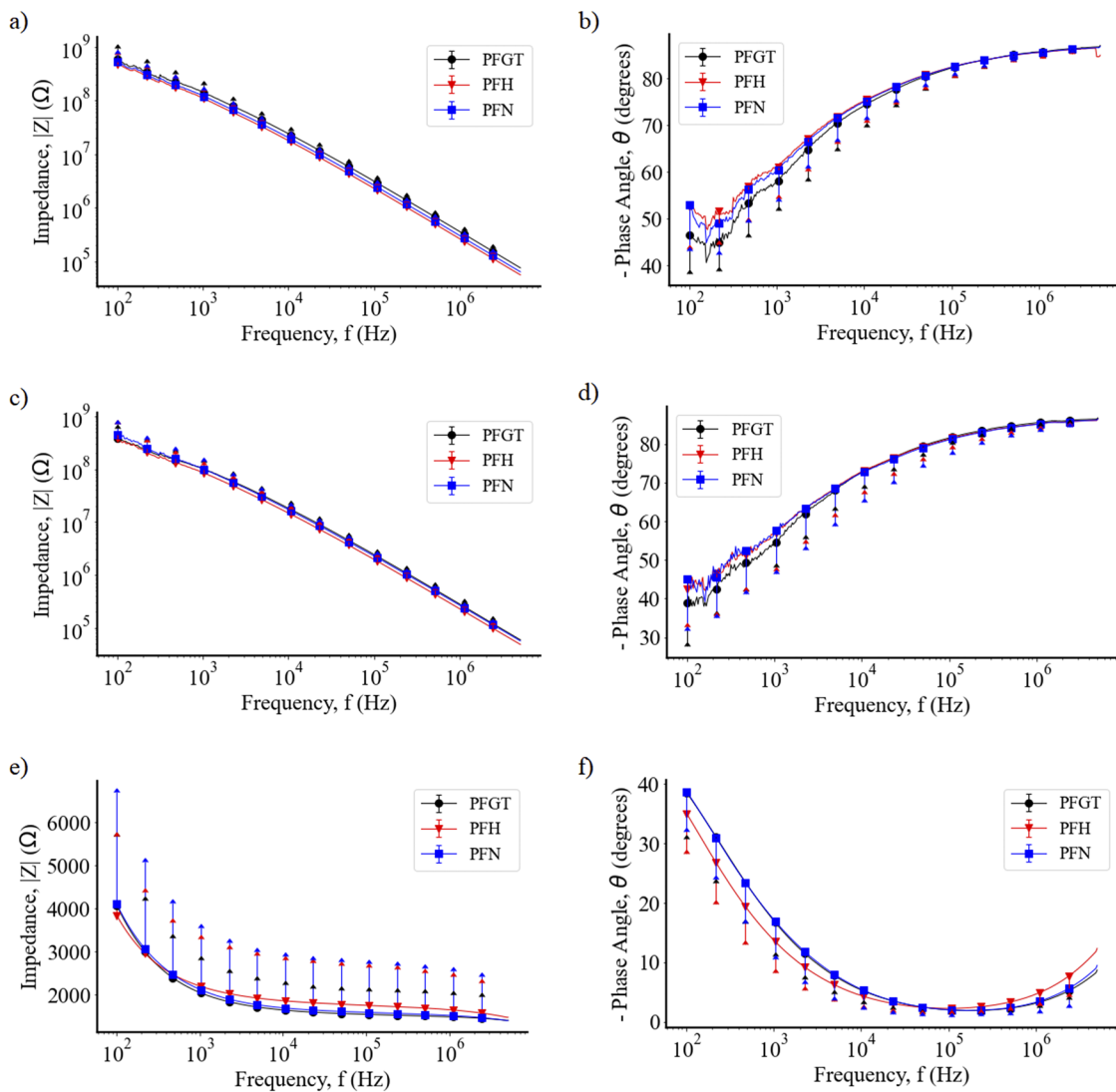
FIG. 3. Mean values and standard deviations of impedance and phase angle for dry samples (a) and (b); for fat-retained samples, i.e., devoid of water but still including fat (c) and (d); and for wet samples, including fat (e) and (f) for different sites of porcine trabecular bone, i.e., PFGH, PFH, and PFN.

PFH and other regions (PFN and PFGT). No significant difference could be observed between PFN and PFGT. Similarly, the associated phases showed obvious difference between PFH and other regions, where the values were higher at frequencies lower than 100 kHz, in comparison with higher frequencies. Phase angles for all the regions were found to be between 36°–40° and 8°–12° at 100 Hz and 5 MHz, respectively. It is worth noting that the values for phase angles were close to 0° for all regions at a frequency of 100 kHz.

B. Dielectric properties

The dielectric properties that were derived from the impedances at higher frequencies—from 1 to 5 MHz—are shown in Fig. 4. The permittivity of dry samples [Fig. 4(a)] slightly decreased with increasing frequency. The different regions could be generally distinguished from each other for the dry and fat-retained samples depending on their individual relative permittivities. All values (and the corresponding standard deviations) for dry samples decreased continuously with increasing frequency for PFH, PFN, and PFGT with mean values in the range from 3.2 to 5.0. Permittivity for fat-retained samples showed a generally similar characteristic but with larger values than those obtained for dry samples, with mean values from 4.0 to 6.0. Despite the overlapping standard deviations, it was possible to also assign wet samples to different regions based on the derived relative permittivities. In this case, greater variations for permittivity were found with mean values from 48–64 at a frequency of 1 MHz and from 28–38 at 5 MHz. The differences were more pronounced for wet than for
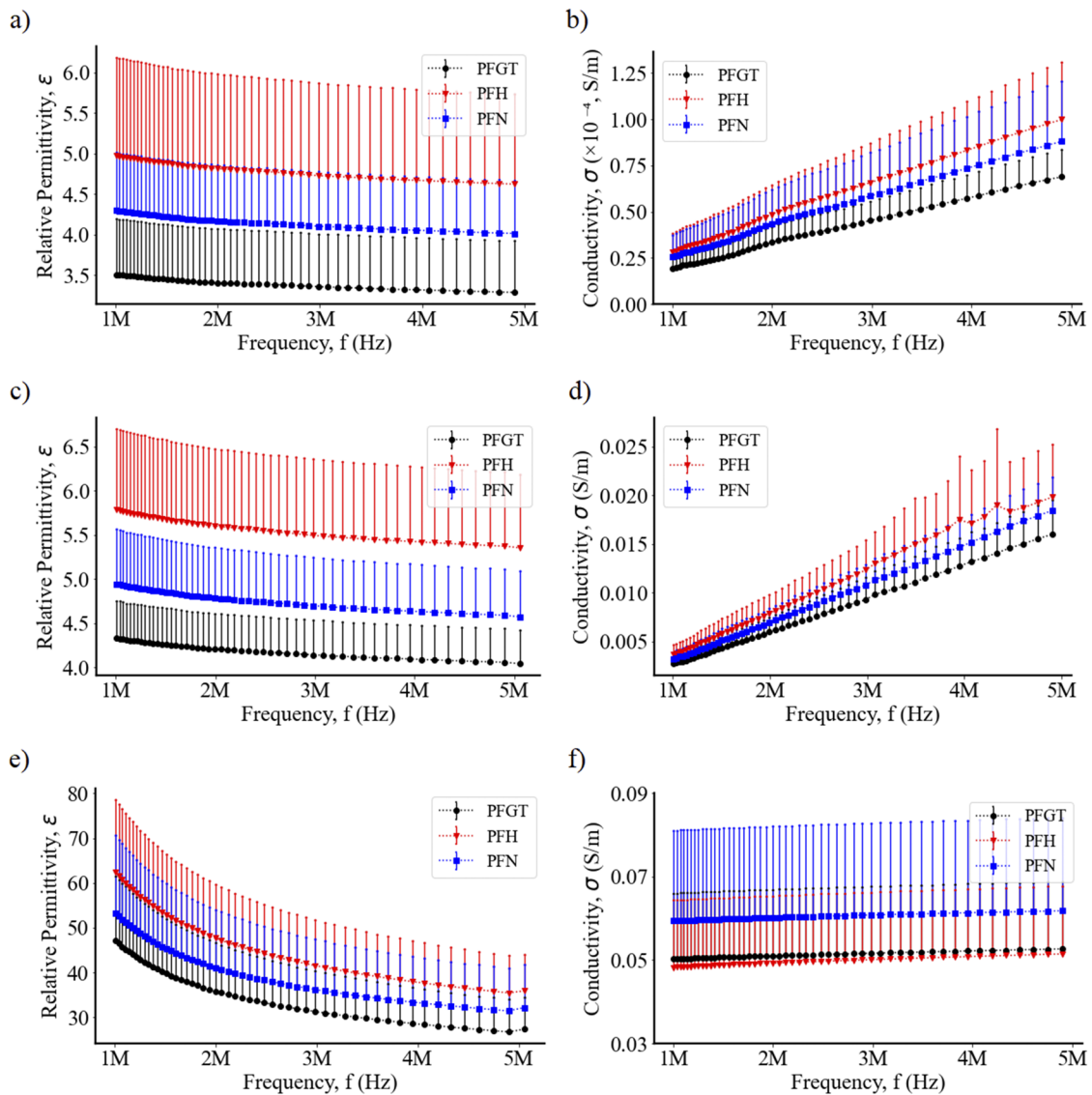
FIG. 4. Relative permittivity and conductivity of dry samples (a) and (b); fat-retained samples, i.e., devoid of water but still including fat (c) and (d); and wet samples, including fat (e) and (f) for different sites of porcine trabecular bone, i.e., PFGH, PFH, and PFN, together with error bars (standard deviations).

dry and fat-retained samples. Similar to the dry and fat-retained samples, PFH had the largest permittivity, followed by PFN and PFGT.

Conductivity of dry bones [Fig. 4(b)] was rather small together with small standard deviations. The mean values for the three regions gradually increased from about 2.5×10^{-5} S/m at 1 MHz to over 6×10^{-5} S/m at 5 MHz. The values for fat-retained samples were much larger than those for dry samples and increased from 0.002 to 0.018 S/m with increasing frequency [Fig. 4(d)], which could be due to the presence of the more conductive fat. With and without fat distinct differences could be established for the different regions,

with the largest mean values obtained for PFH, followed by PFN and PFGT. Conductivities were obviously larger and afflicted with larger standard deviations for wet samples than for dry and fat-retained samples. In comparison with that of dry and fat-retained samples, the conductivity of wet samples [Fig. 4(f)] showed an insignificant increase between 1 and 5 MHz. Mean values for PFN, PFGT, and PFH generally did not deviate much from 0.06, 0.05, and 0.048 S/m, respectively. In particular, the conductivities of PFGT and PFH were rather similar, but both could be clearly distinguished from values for PFN-samples. This supports that conductivity was dominantly determined by even small differences in water content.[30] The

corresponding results are shown in Table II, where water contents of PFGT (0.14 ± 0.02) and PFH (0.13 ± 0.02) were close to each other but distinct from that of PFN (0.18 ± 0.07).

C. Microstructural characterization by the UM-model

The bone volume fraction, BV/TV, was determined with the UM-model for assumed distributions of different constituents (HA, water, fat, and porosity). Given a suitable value of ν, the resulting values for BV/TV were compared with experimental values that were determined from μCT-images to establish the best fitting underlying assumptions for the respective sample. The quality of the fit was expressed by relative errors of the values derived by the UM-model with respect to the experimental μCT-assessment.

To reduce the adverse effect of EP at low frequency,[31] the bone volume fraction, BV/TV, was estimated between 1 and 5 MHz, at which the dielectric properties were predominantly influenced by its intrinsic microstructure and components, i.e., water, fat, porosity, and HA. A very consistent and stable estimation for the underlying distribution was observed for dry samples [Fig. 5(a)] for all regions when HA and porosity were considered as the main components. Corresponding to the results from μCT-images, the estimated BV/TV was the largest for PFH, followed by slightly lower values for PFN and PFGT, which was also the case for fat-retained and wet samples. Results showed that BV/TV estimated by the UM-model for PFH was almost frequency-independent, with values not deviating much from about 0.405 and similar to values of 0.40 ± 0.06
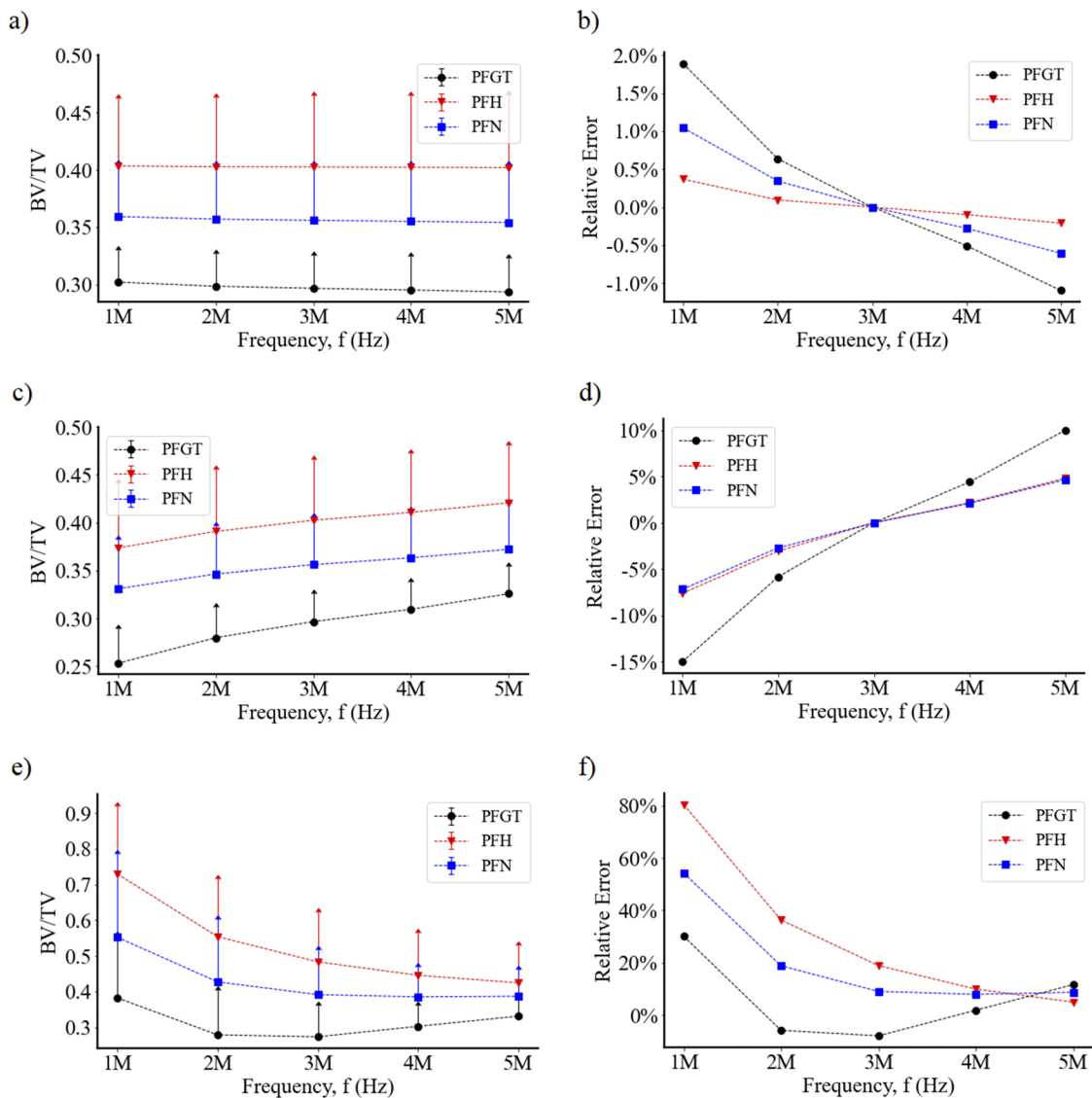

FIG. 5. Bone volume fraction (BV/TV) of dry samples (a), fat-retained samples, i.e., devoid of water but still including fat (c), and wet samples (e) and the corresponding relative error of dry (b), fat-retained (d), and wet samples, including fat (f), with respect to the experimental data determined by μCT.

derived from μCT-images. Only a slight drop in BV/TV from 0.36 at 1 MHz to 0.355 at 5 MHz was predicted by the model for PFN, which was again in good agreement with experimental results for BV/TV, i.e., 0.36 ± 0.05. A small decrease of about 1% was also found for BV/TV for PFGT, still well within the range of the image analysis of 0.29 ± 0.03 with an obviously smaller deviation when compared to PFH and PFN. The agreement between results for BV/TV from the model and from the analysis of μCT-images can be described by the relative errors shown in Fig. 5(b). The relative error was highest for PFGT and smallest for PFN. Values, in general, showed only a small decline of 2% for frequencies increasing from 1 to 5 MHz. Notable was, in particular, the almost absent error between model-results and experimental evaluation for 3 MHz, which suggests, in particular, this frequency as most promising for the assessment of bone microstructure from an impedance analysis. Estimation of BV/TV for fat-retained samples showed an opposite trend in comparison to dry samples, i.e., with the predicted values going up with increasing frequency [Fig. 5(c)] for all regions. Relative errors for PFH and PFN were similar to each other but distinctly smaller for PFGT. Similar to the dry samples, the best estimation of BV/TV for fat-retained samples could be obtained at 3 MHz.

Predictions of the UM-model for values of BV/TV for wet samples were at least for PFN and PFH higher than those for the dry and fat-retained samples, mainly for the lower frequencies [Fig. 5(e)]. Predicted values for BV/TV were decreasing with increasing frequency, especially for PFH, with values dropping from 0.73 at 1 MHz to about 0.46 at 5 MHz, and for PFN changing from 0.56 to ~0.43 for the same frequency range. For both regions, the change was becoming smaller with increasing frequencies and did not change for PFN any more significantly for frequencies of 3 MHz and higher. Interestingly, values were also decreasing first for PFGT from 0.39 at 1 MHz to 0.28 at 3 MHz but then increasing again to 0.35 at 5 MHz. The higher values that were derived for wet samples in comparison to dry samples from the UM-model and, therefore, the discrepancy with the reference values from the analysis of μCT-images were also reflected by relative errors that were an order of magnitude larger [Fig. 5(f)], especially at frequencies of 1 and 2 MHz. At 1 MHz, the relative error was as high as 0.8 for PFH and 0.55 and 0.30 for PFN and PFGT, respectively. Notable small errors were again achieved for higher frequencies, especially about 0.4 for PFGT at 3 MHz and generally on the order of 0.1 for all regions at 4 MHz. This again points out this frequency range as most suitable for derivation of microstructure from impedance analysis by the UM-model. This is particularly important with respect to the evaluation of wet samples, which has been considered here as a first step of the approach for future *in vivo* applications where bodily fluids that are represented here by water will have a major effect on measurements and analysis.

IV. DISCUSSION

A. Bone analysis from impedance measurements

Bone quality is correlated with composition, including water and fat content, and microstructure. The microstructure is foremost determined by the main mineral constituent of bone, i.e., hydroxyapatite (HA). Especially, fat (and other soft tissue) could rival the share of HA to bone composition, while water (representing bodily fluids) plays a smaller but important role (Table II), which is

reflected in particular in the dielectric properties of bone. The bone status can be characterized by BV/TV, i.e., the ratio of the mineralized bone volume, BV, to the entire (tissue) volume, TV, which indicates bone mass and, indirectly, bone stability. Patients suffering from bone diseases (e.g., osteoporosis or fractures) often exhibit lower BV/TV. Previous studies have already demonstrated that bone composition and BV/TV are reflected in the dielectric parameters of bone tissue, generally assuming linear correlations.[2,30]

Accordingly, the bone microstructure could be successfully predicted from dielectric properties of bone by using different analytical methods. All these methods have limitations and are based on certain assumptions or *a priori* information. Previous studies could show that BV/TV can be derived from impedimetric measurements if the dielectric properties of the constituents are known. However, an instructive comprehensive assessment generally suffered from contradicting linear relationships of BV/TV with dielectric parameters that have been identified in different studies.[2,13,32] Moreover, different compositions and microstructures cannot be necessarily described by a linear correlation at all. Nonetheless, the inherent benefit of these approaches is that a physical meaning is associated with the evaluation, where a distinction by other more general statistical methods, e.g., multivariate analysis such as PCA and LDA, is lacking. Therefore, another standard approach is an interpretation of bulk dielectric properties by individual contributions of their representation in an equivalent circuit model (ECM). An inherent disadvantage of this method is that distributions and interactions of components cannot be easily accounted for. Our own previous work indicated that ECM elements, e.g., Cole parameters, can be used to predict BV/TV, which was associated with water content,[20] but neither microstructure nor distribution of different components could be revealed. In addition, unavoidable fitting errors often limit a clear distinction of the specimen from different anatomical sites. A comprehensive and physically meaningful interpretation of impedance data, hence, requires models that provide a realistic description of anatomical conditions, e.g., bone microstructure and composition, together with an unambiguous correlation with physical parameters, e.g., dielectric properties.

Recently, effective medium approximations (EMAs) have shown that the contributions of bone microstructure and compositions can be described simultaneously and BV/TV can be derived from the dielectric properties of bone.[16,29] However, the assessment was either purely theoretical, e.g., based on simulations,[29] or a meaningful comparison with experimental data, and the distinction of different anatomical sites was missing sufficient sample numbers.[16] To establish a convincing association of BV/TV with composition and dielectric properties, EMA-models had to be explored further. The unified mixing (UM) model developed here showed diagnostic potential for impedimetric measurements by considering the weighted contribution of different compositions. Inclusions and the environment were considered isotropic and spherical matter. In addition, possible interactions between components could be included.

B. Impedance and dielectric characteristics of trabecular bones

The impedance properties of bone tissues are crucial for the interpretation of its microstructure as the former is affected by the

latter. Previous studies suggested impedance at frequencies in the MHz-range as particularly interesting for clinical applications.[12,33,34] This is primarily due to the dominant role of microstructure and bone constituents for the bulk properties as a significant association was especially observed for higher frequencies (≥1 MHz). Consequently, several previous studies were already dedicated to uncover possible correlations between the microstructure and composition with impedance properties.[12,13,30,33–35] Therefore, impedance characteristics were also meticulously studied here for frequencies from 100 Hz to 5 MHz.

Accurate impedance measurements with small errors were a perquisite for the interpretation by the UM-model. Not surprisingly, the impedance of dry [Fig. 3(a)] and fat-retained samples [Fig. 3(c)] was much higher than that for wet samples [Fig. 3(e)]. At frequencies in the kHz-range, wet samples tend to be affected by EP due to the electrical double layer at the interfaces of the measurement-electrodes and samples.[31] The effect is known to complicate the interpretation of the intrinsic impedance characteristics of bone tissues. This was not an issue for dry and fat-retained samples since most of the free water could be removed. It should be mentioned that bound water that cannot be easily removed might still have persisted in the ultra-, nano-, and even molecular structure.[36] In addition, the properties at low frequency could be affected by the piezoelectric effects from mechanical stress imposed by the electrodes.[37] Dry samples [Fig. 3(b)] were conceivably more resistive than wet samples [Fig. 3(f)]. This confirmed that HA was the decisive contribution. In contrast, the impedance of wet bone at high frequencies (≥1 MHz) was dominated by the interfacial polarization on interfaces of the microstructure, i.e., between water and HA or fat. Accordingly, the impedance expressed the characteristics of bone better at these higher frequencies than at lower frequencies (<1 MHz).

The dielectric properties, e.g., relative permittivity and conductivity, which were derived from impedance measurements, were more indicative for differences between samples of different statuses (Fig. 4) than the actual recorded impedance values. These material attributes were, in particular, independent of geometrical constraints. In addition, results especially obtained for higher frequencies (≥1 MHz) were characteristic of differences of osseous tissues. A previous study has suggested that water content is the primary determinant of conductivity of trabecular bone.[30] Differences in conductivity were observed for the different regions for both dry [Fig. 4(c)] and wet samples [Fig. 4(d)] and were determined by the respective differences of either water content ($p \leq 0.01$) or BV/TV ($p \leq 0.01$). At lower frequencies, the permittivity of wet samples was significantly affected by contributions from electrode polarization and piezoelectric effects (data not shown). Water and fat contet determine the dielectric properties also at higher frequencies[9,30] However, respective parameters were determined by relaxation processes for specific distributions of the constituents. This becomes obvious for the much larger values of permittivity and conductivity of wet samples than fat-retained samples and completely dry samples. Devoid of water, the relative permittivities of dry samples were also more stable, i.e., with smaller variations. The even larger values of dielectric parameters for fat-retained samples, than dry samples, demonstrated the important contribution from fat content. Accordingly, an obvious distinction of different anatomical sites was possible for dry, fat-retained, and wet samples, which was reflected

in the non-overlapping mean values of permittivities. This discrimination was again more prominent for dry samples [Fig. 4(a)] than for wet samples [Fig. 4(b)] at higher frequencies and emphasized the role of the main constituent of the bone matrix, i.e., HA. This also recommended the permittivity at higher frequencies for an indicative correlation with the bone microstructure as expressed by BV/TV. Permittivity and conductivity changed consistently with increasing BV/TV for all the investigated anatomical regions. Higher values of BV/TV were reflected by likewise higher values of dielectric parameters, which were more significant for permittivity than for conductivity. This suggested permittivity rather than conductivity for use by a UM-model, which was usually also the case for other EMA-models. Accordingly, microstructural information, specifically BV/TV, was derived from the UM-model by considering different components and their respective permittivity. Moreover, contributions could be weighted with respect to the observed bulk permittivity. It should be noted that differences in composition and microstructure cannot be described in a similar fashion simultaneously by an ECM or a statistical analysis.

C. Prediction of microstructure (BV/TV) based on the UM-model

Attention to the actual contribution of different constituents, i.e., water, fat, or porosity, considered as inclusions in an environment, i.e., hydroxyapatite, is the inherent advantage of the model with respect to the description of the bone status. This is notably different from other approaches, such as ECM or multivariate analysis, which are in addition either prone to fitting errors or devoid of physical meaning. Based on the underlying assumptions for the composition, bone can be treated as a homogeneous system, and information on the microstructure (BV/TV) can be determined. The comparison with experimental data from impedance measurements confirms the quality of assumptions and conclusions.

Predictions of BV/TV from the dielectric properties of bone based on a UM-model depend, in particular, on the dimensionless factor v, which rates polarization processes for different inclusions, i.e., components, in a specific environment.[19] Other more specific models implied *a priori* fixed values, e.g., the MG-model ($v = 1$), the Bruggeman model ($v = 2$), and coherent potential approximation ($v = 3$). However, better approximations can be achieved based on less restrictive values in a more general approach. Accordingly, by determining an appropriate value of v, BV/TV could be derived more accurately from the dielectric properties of the significant individual components of bone tissue, i.e., HA, water, and fat. Other content, such as collagen, was not yet considered. The estimated BV/TV was comparable with the experimental values determined by μCT.

The model was, in particular, successful for permittivities that were determined at higher frequencies, e.g., 4 MHz for wet samples and 3 MHz for both dry and fat-retained samples. Larger errors for wet samples indicated, once more, the impact of inclusions filled with water with a much higher relative permittivity. The polarization of macromolecules, such as proteins and collagen,[9] can be described in the UM-model by the parameter v only to some extent, other than the polarization of water and other components. However, with increasing heterogeneity, i.e., more components, such as fat and air, polarization and interaction mechanisms between inclusions of variable size and with different volume fractions are becoming

more complex. Consequently, a less clear correlation was observed between ν and BV/TV for wet bone samples. In this case, estimations of BV/TV were prone to larger errors [Fig. 5(e)]. Conversely, prediction for BV/TV was more precise for samples without water [dry and fat-retained samples, Figs. 5(a) and 5(c)]. Compared with wet samples, fewer components had to be considered, and respective polarization processes became less pronounced. This is most obvious for the simplest system (dry samples) that included only air (reflecting porosity) and HA, where a rather stable estimation of BV/TV [Fig. 5(a)] was obtained with the corresponding highest precision [Fig. 5(b)]. This was demonstrated by the stable estimation of BV/TV at different frequencies and an associated distinct linear correlation with ν ($p < 0.01$) for all investigated anatomical regions, see the example in th eSupplementary Material (Fig. S1). In the absence of water, interfacial polarization became negligible, and only non-conductive HA contributed to the dielectric properties. This permitted an accurate distinction of dry samples from different anatomical regions and resulted in a strong correlation between ν and BV/TV, as further described in the supplementary material (Fig. S1). Notably, BV/TV [Figs. 5(a), 5(c), and 5(e)] and permittivity [Figs. 4(a), 4(c), and 4(e)] estimated by the model agreed with the experimental results and followed the same gradation: largest values for PFH, followed by PFN and eventually PFGT. Correspondingly, a higher HA-content was directly expressed in larger permittivity and could be accurately predicted from this parameter. A similar distinction of different regions was also shown by our previous study for the correlation between water content and the Cole parameter R_∞ (resistance at high frequency).[20] The study already pointed indirectly toward the impedimetric influence of voids for the bone microstructure in relation to BV/TV. However, these voids in the previous study were only filled with a conductive component, i.e., water, while other components, such as fat or HA, had not been considered; porosity has not been explicitly calculated. Since the bone is a highly inhomogeneous and anisotropic material, these characteristics, including the respective effect of interactions between different components on the derivation by the UM-model, should be considered in more detail with respect to the derivation of BV/TV. It is possible that relaxation processes are more involved especially at higher frequencies.

While the UM-model requires information on the relative permittivity (or the conductivity) of the individual components, e.g., 80 for water and 43 for fat, global values, for example, for the bulk permittivity of a composite material, could also be derived from the UM-model at the frequency where BV/TV was predicted with the highest precision, provided an appropriate assumption for ν. Figure S2 illustrates this approach for the determination of the permittivity for dry samples at the "best" frequency of 3 MHz. Small relative errors, close to zero, can also be obtained with this optimal ν of 2.184 $\pm$ 0.027 for fat-retained samples. Conversely, relative errors for wet samples were on the order of about 10% of values that were derived for the permittivity (data not shown).

To investigate how different water and fat content would contribute to the permittivity of wet bones (ε_{eff}), an ideal model that was limited to only water or fat as an additional component [Eqs. (S1) and (S2)] was considered. In this case, values for ν were adopted from PFH-samples for 4 MHz where the relative error between estimated and experimental BV/TV was the smallest [Fig. 5(f)]. Results showed that the change in ε_{eff} ($\Delta\varepsilon_{eff}$), which was caused by water,

was always much greater than that by fat-content (Fig. S3). This shows that despite the generally smaller fraction (Table II), water affected the analysis more strongly than a larger fat-component. This is similarly known for β-dispersions in general, where water also contributes significantly to the dielectric response.[38]

The UM-model facilitates the understanding and determination of the microstructural information of osseous tissue. Together with EIS, the model enables, in particular, to interpret the contribution of individual components to the bulk dielectric properties. In the present study, these were dominated by water content. Admittedly, no other components than either water or fat were included. Therefore, some factors might have been overlooked despite the good agreement with the μCT-image analysis. A possible way to improve the model would be the introduction of additional parameters to "correct" the effect of interactions, which should be a focus of further studies.

V. CONCLUSION

Microstructure and individual components of osseous tissue could be adequately described by the UM-model. Possible interactions between components (hydroxyapatite, water, fat, and porosity) were addressed by the parameter ν, which can be obtained with high accuracy at specific frequencies, i.e., 3 MHz for dry samples and 4 MHz for wet samples. To improve the analysis for wet tissue, contributions of other components and their interactions as well as the effects of dispersions should be included in further developments of the model.

With respect to electrical impedance spectroscopy, the UM-model has been proven as an effective approach to provide meaningful predictive information about the "quality" of bone tissue from dielectric parameters. Impedance properties could be related to bone microstructures that allowed distinguishing even otherwise rather similar samples. This could provide new possibilities for clinical applications. The advantages of the diagnosis of bone quality by real-time, non-radiative, and potentially minimal or non-invasive EIS-measurements are eminent. The approach offers respective advantages for the diagnosis and detection of different osteopathic diseases and even their treatment. Since the dielectric properties inherently determine the distribution of current pathways and local electric fields, the respective evaluation could guide, in particular, the bone remodeling process via electrical stimulation.[33]

SUPPLEMENTARY MATERIAL

See the supplementary material for the comprehensive characterization and understanding of osseous tissues by the UM-model and EIS.

ACKNOWLEDGMENTS

AUTHOR DECLARATIONS

Conflict of Interest

The authors have no conflicts to disclose.

Ethics Approval

DATA AVAILABILITY

The data that support the findings of this study are available within the article and its supplementary material.

REFERENCES

[1] M. C. Lin et al., "Smart bone plates can monitor fracture healing," Sci. Rep. 9(1), 2122 (2019).

[2] T. W. Balmer et al., "Characterization of the electrical conductivity of bone and its correlation to osseous structure," Sci. Rep. 8(1), 8601 (2018).

[3] B. Amin et al., "Dielectric properties of bones for the monitoring of osteoporosis," Med. Biol. Eng. Comput. 57(1), 1–13 (2019).

[4] M. A. Salvino da Silva et al., "A bioimpedance spectroscopy technique to monitor bioprocess involving complex growth micro-organisms," AIP Adv. 11(6), 065032 (2021).

[5] D. Muramatsu, "NaCl-based blood phantom analysis for in vitro bioimpedance measurement," AIP Adv. 11(8), 085301 (2021).

[6] A. H. Alomari, M.-L. Wille, and C. M. Langton, "Bone volume fraction and structural parameters for estimation of mechanical stiffness and failure load of human cancellous bone samples; in-vitro comparison of ultrasound transit time spectroscopy and X-ray μCT," Bone 107, 145–153 (2018).

[7] I. Tamimi et al., "Composition and characteristics of trabecular bone in osteoporosis and osteoarthritis," Bone 140, 115558 (2020).

[8] R. D. Butler and R. J. Halter, "Gauging electrical properties of bone with a bioimpedance-sensing drill," Physiol. Meas. 40(1), 01NT01 (2019).

[9] P. Bhardwaj et al., "Potential of electrical impedance spectroscopy to differentiate between healthy and osteopenic bone," Clin. Biomech. 57, 81–88 (2018).

[10] F. Shi and J. F. Kolb, "Enhanced resolution impedimetric analysis of cell responses from the distribution of relaxation times," Biosens. Bioelectron. 157, 112149 (2020).

[11] E. T. McAdams and J. Jossinet, "Problems in equivalent circuit modelling of the electrical properties of biological tissues," Bioelectrochem. Bioenerg. 40(2), 147–152 (1996).

[12] M. Unal et al., "Interrelationships between electrical, mechanical and hydration properties of cortical bone," J. Mech. Behav. Biomed. Mater. 77, 12–23 (2018).

[13] J. Sierpowska et al., "Interrelationships between electrical properties and microstructure of human trabecular bone," Phys. Med. Biol. 51(20), 5289 (2006).

[14] P. M. Meaney et al., "Bone dielectric property variation as a function of mineralization at microwave frequencies," Int. J. Biomed. 2012, 649612.

[15] B. Amin et al., "Dielectric characterization of diseased human trabecular bones at microwave frequency," Med. Eng. Phys. 78, 21–28 (2020); available at https://www.sciencedirect.com/science/article/pii/S1350453320300254.

[16] I. V. Ciuchi, C. S. Olariu, and L. Mitoseriu, "Determination of bone mineral volume fraction using impedance analysis and Bruggeman model," Mater. Sci. Eng., B 178(19), 1296–1302 (2013).

[17] D. A. G. Bruggeman, "Berechnung verschiedener physikalischer konstanten von heterogenen substanzen. I. Dielektrizitätskonstanten und leitfähigkeiten der mischkörper aus isotropen substanzen," Ann. Phys. 416(7), 636–664 (1935).

[18] L. Jylhä, Ph.D. thesis, Science in Technology, Helsinki University of Technology, 2008.

[19] A. H. Shivola, "Self-consistency aspects of dielectric mixing theories," IEEE Trans. Geosci. Remote Sens. 27(4), 403–415 (1989).

[20] W. Wei, F. Shi, and J. Kolb, "Impedimetric analysis of trabecular bone based on Cole and linear discriminant analysis," Front. Phys. 8, 662 (2020).

[21] Skyscan, SkyScan NRecon user manual, 2011.

[22] Skyscan, Manual for skyscan CT-Analyzer (version 1.10), 2010.

[23] Agilent, Agilent 4294A precision impedance analyzer operational manual, 2003.

[24] C. R. Bowen et al., "Dielectric and piezoelectric properties of hydroxyapatite-BaTiO$_3$ composites," Appl. Phys. Lett. 89(13), 132906 (2006).

[25] P. A. Hasgall et al., IT'IS Database for thermal and electromagnetic parameters of biological tissues, http://www.itis.swiss/database, May 15, 2018.

[26] U. Kaatze, "Complex permittivity of water as a function of frequency and temperature," J. Chem. Eng. Data 34(4), 371–374 (1989).

[27] M. Wang and N. Pan, "Predictions of effective physical properties of complex multiphase materials," Mater. Sci. Eng. R: Rep. 63(1), 1–30 (2008).

[28] S. W. Smye et al., "Modelling the electrical properties of tissue as a porous medium," Phys. Med. Biol. 52(23), 7007 (2007).

[29] R. M. Irastorza, C. M. Carlevaro, and F. Vericat, "Is there any information on micro-structure in microwave tomography of bone tissue?," Med. Eng. Phys. 35(8), 1173–1180 (2013).

[30] J. Sierpowska et al., "Effect of human trabecular bone composition on its electrical properties," Med. Eng. Phys. 29(8), 845–852 (2007).

[31] P. B. Ishai et al., "Electrode polarization in dielectric measurements: A review," Meas. Sci. Technol. 24(10), 102001 (2013).

[32] R. M. Irastorza et al., "Modeling of the dielectric properties of trabecular bone samples at microwave frequency," Med. Biol. Eng. Comput. 52(5), 439–447 (2014).

[33] P. A. Williams and S. Saha, "The electrical and dielectric properties of human bone tissue and their relationship with density and bone mineral content," Ann. Biomed. Eng. 24(2), 222–233 (1996).

[34] D. A. Chakkalakal et al., "Dielectric properties of fluid-saturated bone," IEEE. Trans. Biomed. Eng. BME-27(2), 95–100 (1980).

[35] S. Singh and J. Beharl, "Frequency dependence of electrical properties of human bone," J. Bioelectr. 3(1-2), 347–356 (1984).

[36] M. Granke, M. D. Does, and J. S. Nyman, "The role of water compartments in the material properties of cortical bone," Calcif. Tissue Int. 97(3), 292–307 (2015).

[37] I. V. Ciuchi, "Impedance spectroscopy characterization of bone tissues," J. Adv. Res. Phys. 1(1), 011007 (2010); available at https://stoner.phys.uaic.ro/jarp/index.php?journal=jarp & page=article & op=view & path%5B%5D=8.

[38] W. Kuang and S. O. Nelson, "Low-frequency dielectric properties of biological tissues: A review with some new insights," Trans. ASAE 41, 173–184 (1998).